

Article

CO₂ Adsorption Property of Amine-Modified Amorphous TiO₂ Nanoparticles with a High Surface Area

Misaki Ota * , Yuichiro Hirota , Yoshiaki Uchida and Norikazu Nishiyama

Division of Chemical Engineering, Graduate School of Engineering Science, Osaka University, 1-3 Machikaneyama, Toyonaka, Osaka 560-8531, Japan; yhirota@cheng.es.osaka-u.ac.jp (Y.H.); yuchida@cheng.es.osaka-u.ac.jp (Y.U.); nishiyama@cheng.es.osaka-u.ac.jp (N.N.)

* Correspondence: otam@cheng.es.osaka-u.ac.jp; Tel.: +81-6-6850-6257

Received: 23 May 2018; Accepted: 3 July 2018; Published: 5 July 2018



Abstract: Carbon dioxide capture and storage (CCS) technologies have attracted a great deal of attention as effective measures to prevent global warming. Adsorption methods using porous materials seem to have several advantages over the liquid absorption methods. In this study, we have developed a synthesis method of new amorphous titanium dioxide (TiO₂) nanoparticles with a diameter of 3 nm, a high surface area of 617 m²/g and a large amount of OH groups. Next, the surface of the amorphous TiO₂ nanoparticles was modified using ethylenediamine to examine whether CO₂ adsorption increases. Amorphous TiO₂ nanoparticles were successfully modified with ethylenediamine, which was used in excess due to the presence of a large amount of hydroxyl groups. The amorphous TiO₂ nanoparticles modified with ethylenediamine show a higher CO₂ adsorption capacity (65 cm³/g at 0 °C, 100 kPa) than conventional TiO₂ and mesoporous SiO₂. We discuss the origin of the higher CO₂ adsorption capacity in terms of the high specific surface area of the amorphous TiO₂ nanoparticles and the modification with ethylenediamine on the surface of the amorphous TiO₂ nanoparticles. The optimization of the amount of ethylenediamine bound on the particles increased the CO₂ adsorption capacity without pore blocking.

Keywords: titanium dioxide; amorphous; nanoparticles; ethylenediamine modification; CO₂ adsorption

1. Introduction

Carbon dioxide capture and storage (CCS) technologies have been well studied over the last decade to decrease CO₂ emission in the atmosphere which might contribute to global warming. Various CCS methods including solvent absorption, membrane separation, cryogenics fractionation and adsorption using solid adsorbents have been proposed and developed so far [1–4]. Currently, a liquid phase absorption method using amine (e.g., monoethanolamine) solution has been put into practical use [5]. However, this process has several problems such as corrosion of equipment, degradation of the solution, and, in addition, it requires heat regeneration. Meanwhile, adsorption methods using solid porous materials have attracted more attention over the liquid method [4]. For instance, the adsorption process has higher cycle stability and does not cause corrosion of equipment. Moreover, the adsorption process by using pressure differences is of advantage to the reduction of energy consumption for CO₂ regeneration.

Porous materials including mesoporous alumina, silica, activated carbon and zeolites [6–9] have been studied because these solid adsorbent materials have high surface areas. Moreover, to improve CO₂ adsorption capacity, surface modification of the porous materials has been studied, including amine modification [10–17]. By using the amine-modified porous adsorbents, we can expect an

advantage of the chemical adsorption in addition to the physical adsorption, which arises from chemical reactions between the amine groups and CO₂.

Titanium dioxide has attracted the attention of researchers because of its remarkable properties. It has been applied to photocatalyst and dye-sensitized solar cells [18,19]. In order to improve these functions, many studies have been reported on controlling the structure of TiO₂ and increasing the surface area. The reported TiO₂ has a large variety of structures such as particulate, tube, rod, sheet, and sponge [20–25]. Although these many structures of TiO₂ with high surface area have been reported, there have been fewer reports that amine-modified TiO₂ is applied to CO₂ adsorbents compared to the other porous materials such as SiO₂ [26–31]. This is because TiO₂ generally has small amount of OH groups on the surface to adsorb the amine species and it has been difficult for TiO₂ to be modified with large amount of amines. Amine modification on the TiO₂ requires the presence of OH groups on the surface.

We have developed a synthesis method of new amorphous TiO₂ nanoparticles with high surface area and with higher concentration of OH groups. The amorphous TiO₂ is more reactive with cations such as Li⁺ compared to conventional anatase and rutile crystal TiO₂. The amorphous TiO₂ nanoparticles having OH groups and a high surface area, is considered to enable to be modified with amine used in excess. In this study, we describe the modification of the amorphous TiO₂ nanoparticles with ethylenediamine and their CO₂ adsorption capacity.

2. Materials and Methods

2.1. Synthesis of Amorphous TiO₂ Nanoparticles

According to our previous report [32], 1.4 mL of titanium tetraisopropoxide (TTIP) was mixed with 30 mL of THF and the mixture was stirred at room temperature for 1 h. Next, 1.6 mL of water was added to cause hydrolysis reactions and white precipitates of TiO₂ was immediately formed. Finally, amorphous TiO₂ was collected by centrifugation and dried at 90 °C. The sample is labeled as a-TiO₂-THF. As a reference, we prepared commercially available P25-TiO₂ and titanium dioxide synthesized from TTIP without THF solvent. They are labeled as P25-TiO₂ and TiO₂-solventless, respectively.

2.2. Preparation of Amine-Modified TiO₂ Nanoparticles

The titanium dioxide powder was modified with amines by an impregnation process. The TiO₂ samples (0.2 g) were added into 15 mL of 75 wt % ethylenediamine (EDA) solution in ethanol and stirred at room temperature for 3 h. Then the amine-modified samples were centrifuged and washed by using 10 mL of ethanol. After that, they were dried at 90 °C. The final products are labeled as a-TiO₂-THF-EDA, P25-TiO₂-EDA and TiO₂-solventless-EDA, respectively. In addition, mesoporous silica (MCM-41), which had been well studied as a porous support, was also modified with EDA by the same process and it is labeled as MCM-41-EDA.

2.3. Characterization

The crystallinity of the TiO₂ samples were evaluated by an X-ray diffraction (XRD) pattern using PANalytical X'Pert PRO with Cu K α X-ray (1.54 Å). The particle size and the morphology were measured by the transmission electron microscopy (TEM) images which were recorded on Hitachi H800 electron microscope (Tokyo, Japan) at an acceleration voltage at 200 kV. Nitrogen adsorption-desorption isotherms were measured at 77 K using BELSORP-max (MicrotracBEL Corp., Osaka, Japan). The specific surface area was calculated by the Brunauer-Emmett-Teller (BET) method from nitrogen adsorption isotherms. The pore size distribution and pore volume were calculated by the Brunauer-Joyner-Halenda (BJH) method. Fourier transform infrared (FT-IR) spectra were recorded on a Shimadzu IRAffinity-1 (Kyoto, Japan) in transmission mode with a scan number of 100. The amount of EDA loaded on the samples were measured by thermogravimetry (TG) analysis under air atmosphere

at 20–800 °C at a heating rate of 5 °C/min. The adsorption isotherms of CO₂ were measured at 0 °C with BELSORP-max.

3. Results and Discussion

The XRD patterns of P25-TiO₂, TiO₂-solventless and a-TiO₂-THF are shown in Figure 1. The commercial P25-TiO₂ is composed of a mixture of anatase and rutile structures of TiO₂. The TiO₂-solventless sample synthesized without organic solvent of THF exhibited an anatase crystal structure of TiO₂. On the other hand, the sample synthesized with THF did not show any peaks, indicating that a-TiO₂-THF was amorphous phase. A possible reason would be that THF inhibited the formation of TiO₂ crystal structure. The molecules of TTIP were surrounded by the THF molecules in the solvent. Upon addition of water for hydrolysis reaction, the THF molecules would hinder aggregation of TiO₂ particles and particle growth. According to XRD pattern of the TiO₂ samples after amine modification, the XRD diffraction peaks were similar to the ones before amine modification, indicating that the crystal structures was not changed.

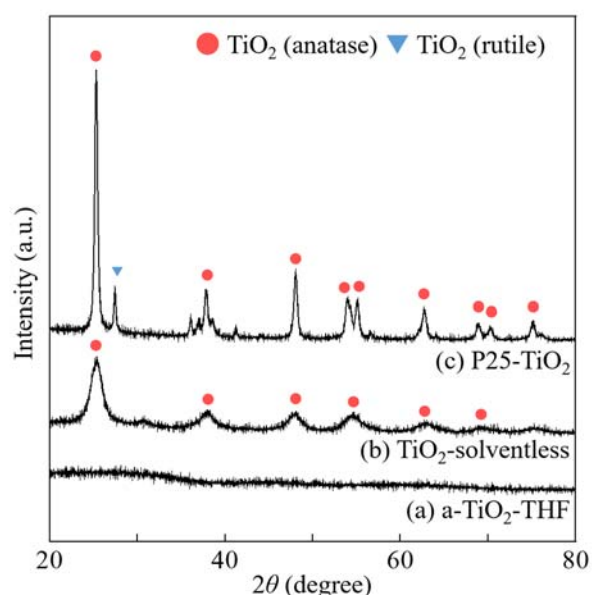


Figure 1. XRD patterns of TiO₂ samples (a) amorphous TiO₂ (b) TiO₂ synthesized without solvent; (c) commercially available P25-TiO₂.

Figure 2 shows TEM images of the TiO₂ samples. Nanoparticles with 3 nm in size were observed for a-TiO₂-THF, while the particle size of TiO₂-solventless and P25-TiO₂ were about 10 and 20–60 nm, respectively. Figure 3 shows N₂ adsorption isotherms and pore size distribution of TiO₂ samples. Their specific surface areas calculated by the BET method from the N₂ adsorption isotherms are summarized in Table 1. The TiO₂ sample synthesized with THF solvent had the highest surface area of about $S_{\text{BET}} = 617 \text{ m}^2/\text{g}$ which is 25 times higher than P25-TiO₂ ($S_{\text{BET}} = 63 \text{ m}^2/\text{g}$). Specific surface area of TiO₂-solventless was $241 \text{ m}^2/\text{g}$. According to N₂ adsorption isotherm, TiO₂-THF showed a high adsorbed amount at low relative pressure suggesting the presence of micropores in addition to mesopores. The high specific surface area of a-TiO₂-THF could be caused by the micropores. When TiO₂-THF was synthesized, the THF molecules could surround TTIP molecules. The THF molecules stabilized TTIP molecules and inhibited the hydrolysis reaction of TTIP. The TiO₂ particles did not grow well, thus smaller nanoparticles were formed. When THF was dried, vacancy from THF molecules would become micropores. On the other hand, TiO₂-solventless and P25-TiO₂ had mesopores and macropores, respectively.

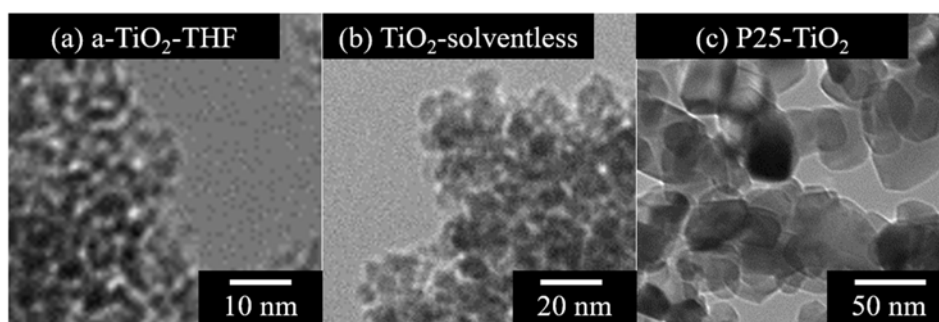


Figure 2. TEM images of TiO₂ samples (a) amorphous TiO₂ (b) TiO₂ synthesized without solvent; (c) commercially available P25-TiO₂.

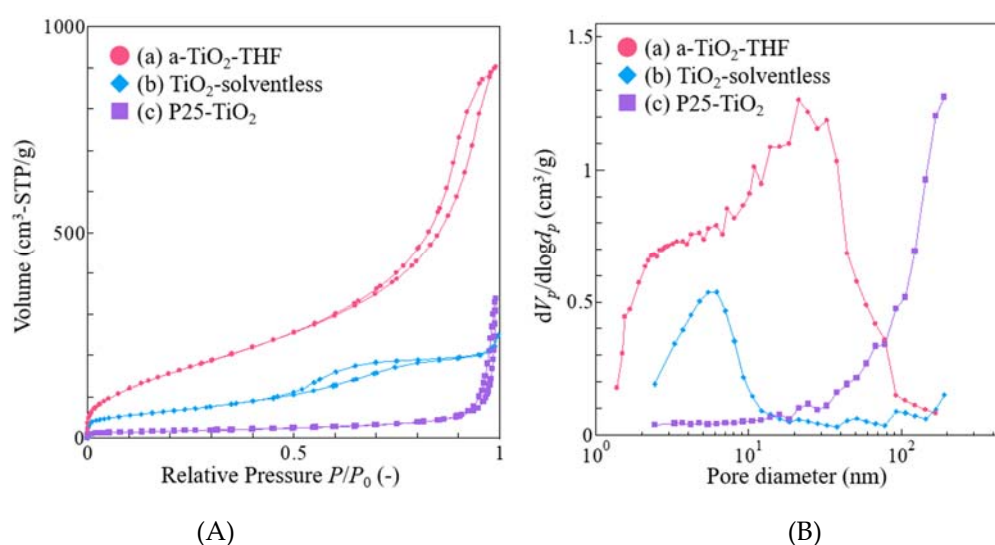


Figure 3. (A) N₂ adsorption/desorption isotherms and (B) pore size distributions of TiO₂ samples (a) amorphous TiO₂ (b) TiO₂ synthesized without solvent (c) commercially available P25-TiO₂.

Table 1. Specific surface area, pore volume and amount of loaded amine of TiO₂ samples and MCM-41.

	S_{BET} (m ² /g)	V (cm ³ /g)	Amount of Loaded Amine (wt %)	Amount of Loaded Amine (mg/m ²)
a-TiO ₂ -THF	617	1.582	-	-
a-TiO ₂ -THF-EDA	472	1.134	15.1	0.245
TiO ₂ -solventless	241	0.356	-	-
TiO ₂ -solventless-EDA	201	0.330	4.7	0.197
P25-TiO ₂	63	0.486	-	-
P25-TiO ₂ -EDA	40	0.502	1.1	0.175
MCM-41	978	0.504	-	-
MCM-41-EDA	360	0.148	12.2	0.125

The specific surface area and pore volume decreased with increasing amount of loaded amine. According to pore size distributions calculated from the nitrogen adsorption isotherms of a-TiO₂-THF-EDA and TiO₂-solventless-EDA after amine modification, the peak did not shift from the samples before amine modification and only the pore volume was reduced (see supporting information Figure S1). This results suggest that TiO₂ was not uniformly modified with EDA on the micropores and mesopores surface, but TiO₂ was rather modified with EDA as if EDA blocked some of the pores.

FT-IR spectra of TiO₂ and TiO₂-EDA samples were measured to confirm the presence of OH groups of TiO₂ and amine modification onto TiO₂ samples, respectively. The absorption peaks at 400–1000 cm⁻¹ of all the samples in Figure 4 were ascribed to lattice vibration of TiO₆ octahedral crystal. The strong absorption peaks at 1630 and around 3400 cm⁻¹ were attributed to the bending vibration and the stretching vibration of O–H bonds, respectively. The peak intensity of a-TiO₂-THF was stronger than TiO₂-solventless and P25-TiO₂, indicating that a-TiO₂-THF samples had more amount of OH groups on the surface than TiO₂-solventless and P25-TiO₂. The peaks attributed C–H and C–O vibration at 2974 cm⁻¹ and 1126 cm⁻¹ respectively were observed for a-TiO₂-THF. These peaks were derived from OC₃H₇ groups of TTIP. The hydrolysis reaction of TTIP to form TiO₂ is as follows:

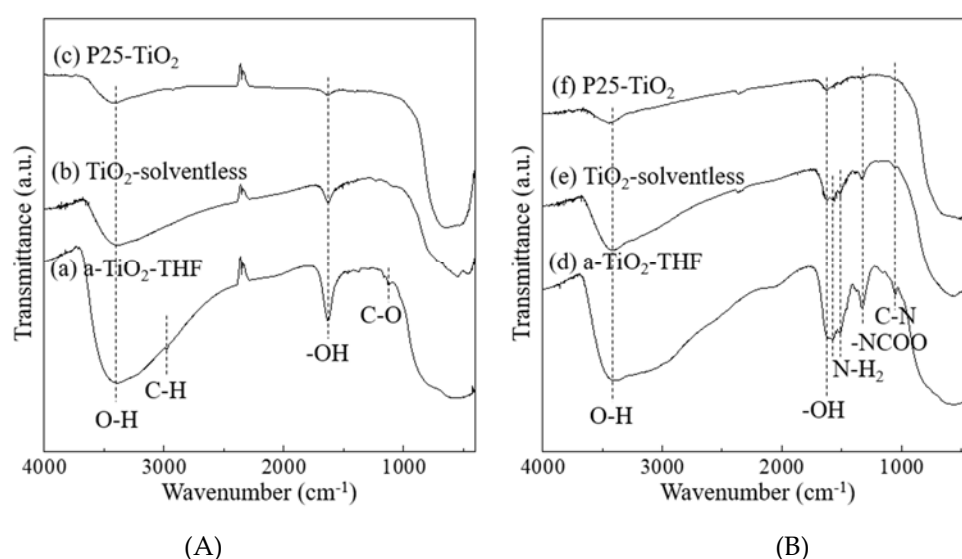
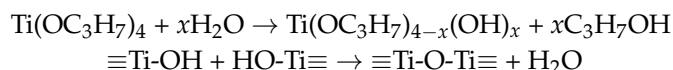


Figure 4. FT-IR spectra of TiO₂ samples (A) before amine modification (a) amorphous TiO₂ (b) TiO₂ synthesized without solvent (c) commercially available P25-TiO₂, and (B) those after amine modification (d) a-TiO₂-THF-EDA (e) TiO₂-solventless-EDA (f) P25-TiO₂-EDA.

When the hydrolysis reaction of TTIP occurred in the presence of the THF solvent, the intermediates Ti(OC₃H₇)_{x-4}(OH)_x were stabilized by an interaction with oxygen atoms of THF molecules. This interaction would be weak but enough to stabilize the intermediates. In consequence, unreacted groups such as OH or OC₃H₇ remained on the surface of nanoparticles after THF was removed by drying.

After EDA modification, the new peaks emerged at 1031, 1515 cm⁻¹ were assigned to C–N stretching vibration and N–H₂ vibration in the primary amine group (RNH₂) respectively, indicating the presence of EDA on the surface of a-TiO₂-THF and TiO₂-solventless. Weak peaks at 1031 cm⁻¹ attributed amine group were observed for P25-TiO₂, indicating that little amounts of amine were loaded on P25-TiO₂ since P25-TiO₂ did not have enough OH groups on the surface for adsorption of amine species. The intensity of the absorption peaks ascribed to OH groups were not much decreased by the EDA modification for all samples, suggesting that OH groups remained from the amine treatment. The absorption peaks at 1330 cm⁻¹ could be ascribed to skeletal vibration of –NCOO by adsorbed gaseous CO₂ in the atmosphere [33].

The specific surface area, pore volume and the amount of EDA loaded on the samples measured by TG analysis were summarized in Table 1 and compared with those from MCM-41. The loaded amount of EDA was 15.1 wt % (a-TiO₂-THF-EDA), 4.7 wt % (TiO₂-solventless-EDA), 1.1 wt % (P25-TiO₂-EDA)

and 12.2 wt % (MCM41-EDA), respectively. Amorphous TiO₂ nanoparticles were modified with the largest amount of amine. One of the reasons seems to be the fact that a-TiO₂-THF has a high specific surface area. Table 1 also shows the values of the loaded amount of amine per surface area. In per unit surface area, amine-modified amount onto a-TiO₂-THF was the highest too. Since there is a large amount of OH groups on the surface of a-TiO₂-THF, many amines could be loaded there.

The adsorption isotherms of CO₂ at 0 °C are shown in Figure 5. The effect of the modification with amine on the enhancement of CO₂ adsorption capacity was more largely for a-TiO₂-THF than TiO₂-solventless and P25-TiO₂. This result is due to the higher contents of OH groups of a-TiO₂-THF than TiO₂-solventless and P25-TiO₂ with anatase and rutile crystal structure. Two schemes of enhanced CO₂ adsorption onto amine-modified material containing Ti and OH groups have been proposed [34]. First, –NH₂ groups of amines react with CO₂ to form carbamate species according to the equation shown below.

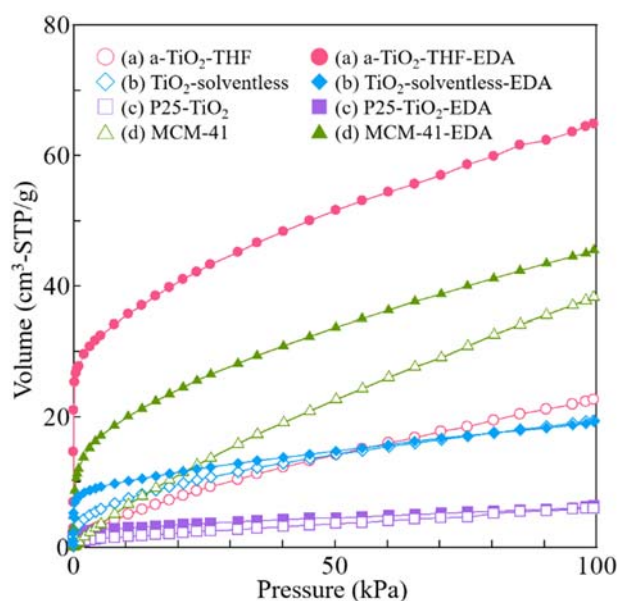


Figure 5. CO₂ adsorption isotherms of TiO₂ samples MCM-41 at 0 °C (open symbols) before amine modification (closed symbols) after amine modification.

Second, CO₂ adsorption is promoted by electrostatic force between CO₂ molecules and amine molecules and –OH groups of TiO₂ surface. The high CO₂ adsorption capacity of a-TiO₂-THF is possibly due to the enhancement of the second scheme because a-TiO₂-THF has high surface area and a high surface concentration of –OH groups. In addition, a-TiO₂-THF-EDA exhibited a higher CO₂ adsorption capacity than MCM-41-EDA even though the specific surface area of a-TiO₂-THF was lower than that of MCM-41 (978 m²/g). In the CO₂ adsorption isotherm, the rise at the low-pressure side is due to adsorption by the reaction of amines and CO₂ described as above the first scheme. Generally, adsorption volume at 20–100 kPa is considered as physical adsorption volume. In that case, the slope of the adsorption isotherms before and after amine modification should be similar at the high pressure side (20–100 kPa). However, the slope of the adsorption isotherm of MCM-41-EDA was smaller than that of the MCM-41. This is possibly because the effective surface area for the physical adsorption was decreased by amine modification. On the other hand, the slope of the adsorption isotherm of a-TiO₂-THF sample was not decreased and rather increased. The improvement of adsorption capacity can be explained by the above second scheme. The OH groups should be exposed on the surface. Therefore, with regard to the MCM-41 which had few OH groups (see supporting information Figure S2), the physical adsorption mainly occurs. On the other hand, as described above, according to FT-IR

measurement of α -TiO₂-THF, a part of OH groups was present on the surface of TiO₂, which enhances adsorption of the second scheme process. Along with increasing the loaded EDA amount, CO₂ adsorption capacity decreased (see supporting information Figure S3). Excessive amine modification caused a pore blocking which reduces the surface area. In addition, OH groups on the surface was covered with amine molecules. In this study, the optimized amine loading effectively could increase the CO₂ adsorption capacity without pore blocking.

4. Conclusions

This work demonstrates synthesis methods of amorphous TiO₂ nanoparticles with a high surface area and large amount of OH groups. The amorphous TiO₂ nanoparticles were synthesized by using THF as a solvent in hydrolysis reaction of TTIP. According to the results of the TEM observation, the amorphous TiO₂ had particle size of 3 nm, which is the smallest size among the conventional ones. The nitrogen adsorption isotherm had an initial rise derived from the micropores at a low-pressure area. The specific surface area calculated from the nitrogen adsorption isotherm was 617 m²/g, which was 10 times larger than the commercially available P25-TiO₂.

Next, our amorphous TiO₂ nanoparticles were modified by ethylenediamine. For modification of amorphous TiO₂ nanoparticles, amine was used in excess because of not only the high specific surface area but also many OH groups which adsorb amine molecules. The amine-modified amorphous TiO₂ nanoparticles showed the highest CO₂ adsorption capacity among those of the amine-modified TiO₂ supports and mesoporous silica MCM-41. The possible reasons for the high CO₂ adsorption capacity are (1) the high specific surface area of the amorphous TiO₂ nanoparticles which contributes to the physical immobilization with CO₂; (2) the high loading of amine molecules which react with CO₂ effectively and (3) the tripartite hydrogen bonding interactions among the amine molecules, CO₂ and OH groups on the TiO₂ surface. The new amorphous TiO₂ nanoparticles having OH groups and a high surface area is a promising material for CO₂ adsorption.

Supplementary Materials: The following are available online at <http://www.mdpi.com/2504-5377/2/3/25/s1>. Figure S1: Nitrogen adsorption isotherms and pore size distributions after amine modification; Figure S2: FTIR spectra of MCM41; Figure S3: CO₂ adsorption volume at 100 kPa of amine-modified samples synthesized by using various ethylenediamine/ethanol concentration; Figure S4: TG curves of amine-modified samples; Table S1: micro-, meso- and macro pore volume of TiO₂ samples.

Author Contributions: M.O. and N.N. conceived and designed the experiments; M.O. performed the experiments, analyzed the data and wrote the paper; Y.H. and Y.U. contributed to critical revision of the manuscript.

Funding: This work was supported by JSPS KAKENHI Grant Number 16K14458.

Acknowledgments: The TEM measurements were carried out by using a facility in Research Center for Ultrahigh Voltage Electron Microscopy, Osaka University.

Conflicts of Interest: The authors declare no conflict of interest.

References

1. Bonenfant, D.; Mimeault, M.; Hausler, R. Determination of the structural features of distinct amines important for the absorption of CO₂ and regeneration in aqueous solution. *Ind. Eng. Chem. Res.* **2003**, *42*, 3179–3184. [[CrossRef](#)]
2. Xiao, Y.C.; Low, B.T.; Hosseini, S.S.; Chung, T.S.; Paul, D.R. The strategies of molecular architecture and modification of polyimide-based membranes for CO₂ removal from natural gas—A review. *Prog. Polym. Sci.* **2009**, *34*, 561–580. [[CrossRef](#)]
3. Song, C.F.; Kitamura, Y.; Li, S.H. Evaluation of Stirling cooler system for cryogenic CO₂ capture. *Appl. Energy* **2012**, *98*, 491–501. [[CrossRef](#)]
4. Wang, Q.A.; Luo, J.Z.; Zhong, Z.Y.; Borgna, A. CO₂ capture by solid adsorbents and their applications: Current status and new trends. *Energy Environ. Sci.* **2011**, *4*, 42–55. [[CrossRef](#)]
5. Hassan, S.M.N.; Douglas, P.L.; Croiset, E. Techno-economic study of CO₂ capture from an existing cement plant using MEA scrubbing. *Int. J. Green Energy* **2007**, *4*, 197–220. [[CrossRef](#)]

6. Ge, J.R.; Deng, K.J.; Cai, W.Q.; Yu, J.G.; Liu, X.Q.; Zhou, J.B. Effect of structure-directing agents on facile hydrothermal preparation of hierarchical gamma-Al₂O₃ and their adsorption performance toward Cr(VI) and CO₂. *J. Colloid Interface Sci.* **2013**, *401*, 34–39. [[CrossRef](#)] [[PubMed](#)]
7. Hiyoshi, N.; Yogo, K.; Yashima, T. Adsorption characteristics of carbon dioxide on organically functionalized SBA-15. *Microporous Mesoporous Mater.* **2005**, *84*, 357–365. [[CrossRef](#)]
8. Siriwardane, R.V.; Shen, M.S.; Fisher, E.P.; Poston, J.A. Adsorption of CO₂ on molecular sieves and activated carbon. *Energy Fuels* **2001**, *15*, 279–284. [[CrossRef](#)]
9. Lee, J.S.; Kim, J.H.; Kim, J.T.; Suh, J.K.; Lee, J.M.; Lee, C.H. Adsorption equilibria of CO₂ on zeolite 13X and zeolite X/Activated carbon composite. *J. Chem. Eng. Data* **2002**, *47*, 1237–1242. [[CrossRef](#)]
10. Chen, C.; Kim, J.; Ahn, W.S. CO₂ capture by amine-functionalized nanoporous materials: A review. *Korean J. Chem. Eng.* **2014**, *31*, 1919–1934. [[CrossRef](#)]
11. Cai, W.Q.; Tan, L.J.; Yu, J.G.; Jaroniec, M.; Liu, X.Q.; Cheng, B.; Verpoort, F. Synthesis of amino-functionalized mesoporous alumina with enhanced affinity towards Cr(VI) and CO₂. *Chem. Eng. J.* **2014**, *239*, 207–215. [[CrossRef](#)]
12. Le, Y.; Guo, D.P.; Cheng, B.; Yu, J.G. Amine-functionalized monodispersed porous silica microspheres with enhanced CO₂ adsorption performance and good cyclic stability. *J. Colloid Interface Sci.* **2013**, *408*, 173–180. [[CrossRef](#)] [[PubMed](#)]
13. Bali, S.; Leisen, J.; Foo, G.S.; Sievers, C.; Jones, C.W. Aminosilanes Grafted to Basic Alumina as CO₂ Adsorbents-Role of Grafting Conditions on CO₂ Adsorption Properties. *ChemSusChem* **2014**, *7*, 3145–3156. [[CrossRef](#)] [[PubMed](#)]
14. Santos, T.C.D.; Bourrelly, S.; Llewellyn, P.L.; Carneiro, J.W.D.; Ronconi, C.M. Adsorption of CO₂ on amine-functionalised MCM-41: Experimental and theoretical studies. *Phys. Chem. Chem. Phys.* **2015**, *17*, 11095–11102. [[CrossRef](#)] [[PubMed](#)]
15. Liu, J.; Liu, Y.; Wu, Z.B.; Chen, X.B.; Wang, H.Q.; Weng, X.L. Polyethyleneimine functionalized protonated titanate nanotubes as superior carbon dioxide adsorbents. *J. Colloid Interface Sci.* **2012**, *386*, 392–397. [[CrossRef](#)] [[PubMed](#)]
16. Melendez-Ortiz, H.I.; Perera-Mercado, Y.; Mercado-Silva, J.A.; Olivares-Maldonado, Y.; Castruita, G.; Garcia-Cerda, L.A. Functionalization with amine-containing organosilane of mesoporous silica MCM-41 and MCM-48 obtained at room temperature. *Ceram. Int.* **2014**, *40*, 9701–9707. [[CrossRef](#)]
17. Zhu, Y.J.; Zhou, J.H.; Hu, J.; Liu, H.L. The effect of grafted amine group on the adsorption of CO₂ in MCM-41: A molecular simulation. *Catal. Today* **2012**, *194*, 53–59. [[CrossRef](#)]
18. Fujishima, K. Honda, Electrochemical Photolysis of Water at a Semiconductor Electrode. *Nature* **1972**, *238*, 37. [[CrossRef](#)] [[PubMed](#)]
19. Li, B.; Wang, L.; Kang, B.; Wang, P.; Qiu, Y. Review of recent progress in solid-state dye-sensitized solar cells. *Sol. Energy Mater. Sol. Cells* **2006**, *90*, 549–573. [[CrossRef](#)]
20. Fan, J.J.; Zhao, L.; Yu, J.G.; Liu, G. The effect of calcination temperature on the microstructure and photocatalytic activity of TiO₂-based composite nanotubes prepared by an in situ template dissolution method. *Nanoscale* **2012**, *4*, 6597–6603. [[CrossRef](#)] [[PubMed](#)]
21. Yu, J.G.; Dai, G.P.; Cheng, B. Effect of Crystallization Methods on Morphology and Photocatalytic Activity of Anodized TiO₂ Nanotube Array Films. *J. Phys. Chem. C* **2010**, *114*, 19378–19385. [[CrossRef](#)]
22. Yun, H.J.; Lee, H.; Joo, J.B.; Kim, W.; Yi, J. Influence of Aspect Ratio of TiO₂ Nanorods on the Photocatalytic Decomposition of Formic Acid. *J. Phys. Chem. C* **2009**, *113*, 3050–3055. [[CrossRef](#)]
23. Wang, Y.W.; Zhang, L.Z.; Deng, K.J.; Chen, X.Y.; Zou, Z.G. Low temperature synthesis and photocatalytic activity of rutile TiO₂ nanorod superstructures. *J. Phys. Chem. C* **2007**, *111*, 2709–2714. [[CrossRef](#)]
24. Chen, J.S.; Lou, X.W. Anatase TiO₂ nanosheet: An ideal host structure for fast and efficient lithium insertion/extraction. *Electrochem. Commun.* **2009**, *11*, 2332–2335. [[CrossRef](#)]
25. Hoces, M.; Berginc, M.; Topic, M.; Krasovec, U.O. Sponge-like TiO₂ layers for dye-sensitized solar cells. *J. Sol-Gel Sci. Technol.* **2010**, *53*, 647–654. [[CrossRef](#)]
26. Jiang, G.D.; Huang, Q.L.; Kenarsari, S.D.; Hu, X.; Russell, A.G.; Fan, M.H.; Shen, X.D. A new mesoporous amine-TiO₂ based pre-combustion CO₂ capture technology. *Appl. Energy* **2015**, *147*, 214–223. [[CrossRef](#)]
27. Liao, Y.S.; Cao, S.W.; Yuan, Y.P.; Gu, Q.; Zhang, Z.Y.; Xue, C. Efficient CO₂ Capture and Photoreduction by Amine-Functionalized TiO₂. *Chem. Eur. J.* **2014**, *20*, 10220–10222. [[CrossRef](#)] [[PubMed](#)]

28. Kanarsari, S.D.; Fan, M.; Jiang, G.; Shen, X.; Lin, Y.; Hu, X. Use of Robust and Inexpensive Nanoporous TiO₂ for Pre-combustion CO₂ separation. *Energy Fuels* **2013**, *27*, 6938–6947. [[CrossRef](#)]
29. Aquino, C.C.; Richner, G.; Kimling, M.C.; Chen, D.; Puxty, G.; Feron, P.H.M.; Caruso, R.A. Amine-Functionalized Titania-based Porous Structures for Carbon Dioxide Postcombustion Capture. *J. Phys. Chem. C* **2013**, *117*, 9747–9757. [[CrossRef](#)]
30. Muller, K.; Lu, D.; Senanayake, S.D.; Starr, D.E. Monoethanolamine Adsorption on TiO₂(110): Bonding, Structure, and Implications for Use as a Model Solid-Supported CO₂ Capture Material. *J. Phys. Chem. C* **2014**, *18*, 1576–1586. [[CrossRef](#)]
31. Kapica-Kozar, J.; Pirog, E.; Kusiak-Nejman, E.; Weobel, R.J.; Gesikiewicz-Puchalska, A.; Morawski, A.W.; Nakiewicz, U.; Michalkiewicz, B. Titanium dioxide modified with various amines used as sorbents of carbon dioxide. *New J. Chem.* **2017**, *41*, 1549–1557. [[CrossRef](#)]
32. Ota, M.; Dwijaya, B.; Hirota, Y.; Uchida, Y.; Tanaka, S.; Nishiyama, N. Synthesis of Amorphous TiO₂ Nanoparticles with a High Surface Area and Their Transformation to Li₄Ti₅O₁₂ Nanoparticles. *Chem. Lett.* **2016**, *45*, 1285–1287. [[CrossRef](#)]
33. Su, F.S.; Lu, C.Y.; Kuo, S.C.; Zeng, W.T. Adsorption of CO₂ on Amine-Functionalized Y-Type Zeolites. *Energy Fuels* **2010**, *24*, 1441–1448. [[CrossRef](#)]
34. Liu, Y.; Liu, J.; Yao, W.Y.; Cen, W.L.; Wang, H.Q.; Weng, X.L.; Wu, Z.B. The effects of surface acidity on CO₂ adsorption over amine functionalized protonated titanate nanotubes. *RSC Adv.* **2013**, *3*, 18803–18810. [[CrossRef](#)]



© 2018 by the authors. Licensee MDPI, Basel, Switzerland. This article is an open access article distributed under the terms and conditions of the Creative Commons Attribution (CC BY) license (<http://creativecommons.org/licenses/by/4.0/>).